RESEARCH ARTICLE

Early Activation of Apoptosis and Caspase-independent Cell Death Plays an Important Role in Mediating the Cytotoxic and Genotoxic Effects of WP 631 in Ovarian Cancer Cells

Arkadiusz Gajek[1]*, Marta Denel-Bobrowska[1], Aneta Rogalska[1], Barbara Bukowska[1], Janusz Maszewski[2], Agnieszka Marczak[1]

Abstract

The purpose of this study was to provide a detailed explanation of the mechanism of bisanthracycline, WP631 in comparison to doxorubicin (DOX), a first generation anthracycline, currently the most widely used pharmaceutical in clinical oncology. Experiments were performed in SKOV-3 ovarian cancer cells which are otherwise resistant to standard drugs such as cis-platinum and adriamycin. As attention was focused on the ability of WP 631 to induce apoptosis, this was examined using a double staining method with Annexin V and propidium iodide probes, with measurement of the level of intracellular calcium ions and cytosolic cytochrome c. The western blotting technique was performed to confirm PARP cleavage. We also investigated the involvement of caspase activation and DNA degradation (comet assay and immunocytochemical detection of phosphorylated H2AX histones) in the development of apoptotic events. WP 631 demonstrated significantly higher effectiveness as a pro-apoptotic drug than DOX. This was evident in the higher levels of markers of apoptosis, such as the externalization of phosphatidylserine and the elevated level of cytochrome c. An extension of incubation time led to an increase in intracellular calcium levels after treatment with DOX. Lower changes in the calcium content were associated with the influence of WP 631. DOX led to the activation of all tested caspases, 8, 9 and 3, whereas WP 631 only induced an increase in caspase 8 activity after 24h of treatment and consequently led to the cleavage of PARP. The lack of active caspase 3 had no outcome on the single and double-stranded DNA breaks. The obtained results show that WP 631 was considerably more genotoxic towards the investigated cell line than DOX. This effect was especially visible after longer times of incubation. The above detailed studies indicate that WP 631 generates early apoptosis and cell death independent of caspase-3, detected at relatively late time points. The observed differences in the mechanisms of the action of WP631 and DOX suggest that this bisanthracycline can be an effective alternative in ovarian cancer treatment.

Keywords: WP 631 - ovarian cancer cells - anthracyclines - apoptosis - DNA damage - caspases

Asian Pac J Cancer Prev, **16 (18)**, 8503-8512

Introduction

Ovarian cancer is the leading cause of death from gynecological malignances. It is often diagnosed late, at the advanced stages of disease III and IV (Siegel et al., 2013; Sundar et al., 2015; Zhao et al., 2015). Ovarian cancer occurs most commonly in women aged over 50, however, it is well known that this malignancy may also, though rarely, develop in children and adolescents (Chaopotong et al., 2015). Important risk factors include a family history of ovarian or breast cancer and a genetic predisposition such as BRCA1/BRCA2 mutations (Jiménez et al., 2013; Pradjatmo et al., 2014). Currently, routine treatment of ovarian cancer consists of cytoreductive surgery followed by carboplatin, anthracyclines and taxane-based chemotherapy. These conventional methods are, in many cases, ineffective, due to the poor response and adverse effects to chemotherapy, such as multi drug resistance (MDR) (Fujiwara et al., 2013).

Anthracycline antibiotics have been well-known as antitumor agents for a significant period, with the best-characterized members of this group being daunorubicin (DNR) and doxorubicin (DOX). Depending on their chemical structure, anthraquinone drugs are able to kill tumor cells by diverse mechanisms, involving various intracellular targets which contribute to drug-induced toxicity and the induction of apoptosis (Pal et al., 2012). Although the direct effects of anthracycline drugs (such as DOX) on DNA damage have been intensively studied (Szwed et al., 2014; Yang et al., 2014; Wojcik et al., 2015),

*[1]Department of Medical Biophysics, [2]Department of Cytophysiology, Faculty of Biology and Environmental Protection, University of Lodz, Pomorska, Lodz, Poland *For correspondence: arekgajek86@wp.pl*

in the case of novel agents, the sequence of morphological and biochemical events leading to cell death remains unclear.

The objective of our study was to compare the mode of cell death induced by WP 631 - a novel anthracycline analog - with the most widely explored DOX. We also investigated the possible involvement of caspases activation and DNA degradation in the development of apoptotic events and their significance for drug efficiency.

Materials and Methods

Chemicals

DOX was obtained from Sequoia Research Products (Pangbourne, UK). RPMI 1640 medium and fetal bovine serum (FBS) were supplied by Lonza (Basel, Switzerland). Trypsin-EDTA, penicillin and streptomycin, WP 631, Caspase-3 Assay Kit were purchased from Sigma (St. Louis, USA). Fluo-4 NW Assay Kit, Annexin V binding Assay Kit, Caspase-8 and -9 Assay Kits and Cytochrome c Elisa Kit were supplied by Invitrogen (Carlsbad, USA). All other chemicals and solvents were of high analytical grade and were obtained from Sigma or POCH S.A. (Gliwice, Poland).

Cell culture

SKOV-3 cells, obtained from American Type Culture Collection (ATCC, Rockville, USA), were grown as a monolayer with RPMI 1640 medium, supplemented with 10% fetal bovine serum, penicillin (10 U/ml) and streptomycin (50 μg/ml) in standard conditions: 37°C, 100% humidity, the atmosphere being 5% CO_2 and 95% air. The cell viability was systematically controlled using trypan blue (0.4%, Sigma). In all experiments, cells in logarithmic phase of growth were used when their viability was above 95%.

Drug treatment

The cells were removed from monolayer by trypsinization, resuspended in fresh complete medium, centrifuged for 5 min at 200×g and plated into appropriate dishes at the optimal density (described into materials and methods section) for measurements of PS externalization, caspases -3, -8 and -9 activity, comet assay, DNA ladder, PARP cleavage, cytochrome c and intracellular calcium ions level. After 24 h (time necessary to ensure that the cells were in the exponential growth phase), the drugs in their IC_{50} concentrations (270 nM for DOX and 96,5 nM for WP 631) (Rogalska et al., 2011) were added to the dishes and the cells were incubated in a CO_2 incubator for different periods of time (2 - 48 h) depending on the assessment method.

Intracellular calcium ions detection

Intracellular calcium level was determined using the fluorescent probe Fluo-4NW, which is able to cross the plasma membrane of living cells. After entering the cell, Fluo-4NW is converted by cytosolic hydrolases to the active form, having the possibility of binding of calcium ions. As a result of joining of calcium ions, the probe emits fluorescence (λ_{em} =538 nm) after excitation with light of wavelength 485 nm. Cells were plated in 96-well black fluorimetric plates (10^4 cells/well) and then treated with DOX or WP 631 in IC_{50} concentration. After incubation times (2, 4, 24, 48 hours) the growth medium was removed and the cells were washed with PBS in order to eliminate sources of baseline fluorescence. Finally a dye loading solution (Fluo-4-NW dye, 4-[(Dipropylamino)sulfonyl] benzoic acid (Probenecid) - used to inhibit extrusion of the indicator out of the cell by organic anion transporters, Hanks' balanced salt solution (HBSS), 20 mM N-(2-hydroxyethyl)piperazine-N'-(2-ethanesulfonic acid) buffer solution (HEPES)) was added in a volume of 100μl per well and incubated for 30 min in the total darkness at 37°C, and then for next 30 min at room temperature. The measurement was done on Fluoroskan Ascent FL microplate reader (Labsystems, Sweden) using 494 nm excitation and 516 nm emission wavelengths.

Estimation of intracellular cytochrome c

This quantitative sandwich assay technique measures the level of cytochrome c in cytoplasm by using monoclonal antibody specific for cytochrome c, which has been pre-coated onto microplate. The cells were plated ($3x10^6$) in 5 ml of complete culture medium into 100 mm Petri dishes. After 24 h, DOX or WP 631 was added in IC_{50} concentration and the cells were incubated for 4 and 48 h. Next, cells were washed with PBS and re-suspended in ice-cold (4°C) cytosol extraction buffer containing protease inhibitor. Cell lysate was centrifuged at 10000 g for 30 minutes at 4°C. The supernatant (cytosolic fraction) was collected and stored at -80°C. Clarified cytoplasm extracts were added to triplicate wells for determining cellular level of cytochrome c. The reactions were continued for 2 h at room temperature. The plate was washed four times with washing buffer and then incubated for 2 h with cytochrome conjugate (100 μl/well). Next, when the plate was aspirated and washed 4 times, 100 μl substrate solution per well was added and the samples were incubated in total darkness, at room temperature for 30min. The reaction was stopped by the addition of 2N sulfuric acid generating a yellow color, which was recorded at 450 nm with a PowerWave microplate reader (BioTek, USA).

Measurements of phosphatidylserine externalization

In early apoptotic cells, the membrane phospholipid: phosphatidylserine (PS) is translocated from the inner layer of the plasma membrane to the outer layer. Annexin V is a protein that specifically binds to PS. Double staining of cells with Annexin V and propidium iodide was used to assess the first stage of apoptosis. This method is a useful tool for distinguishing viable cells (unstained with either fluorochrome) from apoptotic cells (stained with Annexin V) and necrotic (dead) cells (stained with PI). $5x10^5$ control and drug treated cells were washed with cold PBS and re-suspended in 500μl binding buffer (delivered from producer) that contained 5μl of Annexin V fluorescein isothiocyanate (FITC), 5μl of PI and stained for 15 minutes in room temperature. Finally, at least $3x10^4$ cells were analyzed for FITC and PI fluorescence on a flow cytometer (LSR II, Becton Dickinson). With the use of an Annexin

V- FITC and propidium iodide (PI) double staining regime, three populations of cells were distinguishable in two color flow cytometry: normal cells: Annexin V- FITC negative, PI negative; apoptotic cells: Annexin V- FITC positive, PI negative; dead cells: Annexin V- FITC positive and PI positive, Annexin V- FITC negative and PI positive.

Comet assay

The comet assay was performed under alkaline conditions. SKOV-3 cells treated with DOX or WP 631 were collected at 2, 4, 24 and 48h after culture initiation. Cells were suspended in 0.75% low melting point agarose in PBS, pH 7.4. Next, this suspension (50 μl) was spread on frosted microscope slides precoated with a layer of 1% normal melting agarose. After gelling, the slides were treated with lysing buffer consisting of 2.5 M NaCl, 100 mM EDTA, 1% Triton X-100, 10% DMSO and 10 mM Tris, pH 10 at 4°C for 1h. Slides were then placed in the electrophoresis solution (300 mM NaOH, 1 mM EDTA, pH > 13) for 40 min to allow DNA unwinding. Electrophoresis was carried out at 0.73 V/cm, 300 mA for 30 min. The slides were then neutralized with 0.4 M Tris, pH 7.5 and stained with 2 μg/ml DAPI. All these steps were performed in the dark to prevent additional DNA damage. Fifty randomly selected cells from each slide were measured by image analysis ((Nikon, Tokyo, Japan attached to a COHU 4910 video camera (Cohu, Inc., San Diego, CA) equipped with a UV filter by using the image analysis system, Lucia-Comet v. 4.51 (Laboratory Imaging, Praha, Czech Republic). For a direct comparison of the influence of DOX and WP 631 on DNA damage, the % of DNA in comet tail was chosen.

Detection of caspase-8, -9, -3 activity

SKOV-3 cells were treated with IC_{50} concentration of DOX or WP 631 at various time points (4 - 48 h). Control and drug treated cells were harvested and collected in phosphate buffered saline (PBS) (4 x 10^6 cells/sample), and after short centrifugation at 200 x g cell pellets were kept frozen at -80°C until analysis. Additionally, all cell lysates were pretreated for 1 h with the caspase-3 inhibitor, caspase-8 inhibitor or caspase-9 inhibitor at 60 μM concentration. Caspase-3 and -8 activities were estimated by means of a fluorimetric method with Caspase-3 Z-DEVD-R110 Assay Kit (Molecular Probes, USA) and Ac-IETD-AMC Caspase-8 Assay Kit (Sigma Aldrich, Germany). Caspase-9 activity was measured using colorimetric method with Caspase-9 LEHD-pNA Assay Kit (Molecular Probes, USA). All experiments were made according to manual protocols provided by the producents. Microtiter wells were set in 3 repeats for controls, blanks and drug-treated cells. The measurement was done on a Fluoroskan Ascent FL microplate reader (Labsystems, Sweden), using 355 nm excitation and 450 nm emission wavelengths for estimation caspase-3 activity and 360 nmext / 440 nmem for caspase-8 activity. Detection of caspase-9 activity was recorded at 405 nm with a PowerWave microplate reader (BioTek, USA). Cystein proteases activity was expressed as a ratio of the fluorescence (-3, -8) or absorbance (-9) of the drug-treated samples relative to the corresponding untreated controls taken as 100%. The proper inhibitors were used in the control experiments to confirm that the observed fluorescence in both the control and the drug-treated cells is due to caspase-3, -9, -8 presences in the samples.

Detection of oligonucleosomal DNA fragmentation - DNA ladder

The total cellular DNA was extracted from SKOV-3 cells, untreated and treated with tested compounds up for 4, 24 and 48 h, according to the method described by Gong [9] with some minor modifications. Briefly, cells were washed with phosphate-buffered saline (PBS) and lysed at 37°C for 30 minutes in extraction buffer (0.2 M phosphate-citrate buffer, pH 7.8). The samples were then centrifuged at 1500 g for 10 min. Supernatant, which contained Low Molecular Weight DNA (LMW DNA) was incubated with RNase A (1 mg/ml) and Proteinase K (1 mg/ml) for 30 minutes at 37°C. Electrophoresis was performed using a 1.8% agarose gel in TBE buffer [10 mM Tris-Cl, PH 7.5, 1 mM EDTA]. At the end of electrophoresis the gel was stained with 0.005 mg/ml ethidium bromide (EB) for 30 min. The Sigma PCR Marker was used to analyze the lengths of oligonucleosomal fragments formed during programmed cell death. DNA fragments were visualized under UV fluorescence using In Genius Bio Imaging System.

PARP cleavage

The cells were lysed in cell extraction buffer containing the protease inhibitors cocktail and PMSF (phenylmethanesulfonylfluoride) in accordance with the manufacturer's protocol (Invitrogen). Protein concentration was determined using the Bradford Method. SDS-polyacryamide gel electrophoresis (10%) and transfer of proteins (100μg per lane) to nitrocellulose membranes were performed using standard procedures. To confirm equal loading and transfer, PageRuler Prestained Protein Ladder (Fermentas Inc.) was used. After the blocking of nonspecific sites, membranes were incubated with rabbit monoclonal antibody against PARP-1 at a dilution of 1/5000 (Anti-PARP-1, Millipore). Rabbit anti GAPDH polyclonal antibody were used as internal controls at a dilution of 1/200 (AbD Serotec). Signals were detected using an alkaline phosphatase conjugated secondary antibody (goat anti-rabbit, Millipore) diluted 1/400 and colorimetric detection system (Vector Laboratories, Inc.).

Immunocytochemical detection of γ-phosphorylated H2AX histones

Detection of γ-phosphorylated H2AX histones was carried out according to the method described by Zabka et al. (2013) with minor modification. Cells were seeded into 8-well Falcon Cultureslide. After 24 h, drugs at IC_{50} concentrations were added to the wells. The cells were incubated with drugs for 48 h. At the end of drug treatment, the medium was removed and the cells were fixed for 45 min (4°C) in PBS-buffered 4 % paraformaldehyde. After washing with PBS the slides were preincubated with PBS-buffered 8 % bovine serum albumin (BSA) and 4 % Triton X-100 at room temperature for 50 min. In the next step, after washing with PBS, the slides were incubated

for 12 h in a humidified atmosphere (4°C) with rabbit polyclonal antibody raised against human H2AX histones phosphorylated at Ser139 at a dilution of 1 : 750 dissolved in PBS containing 1 % BSA. After washing with PBS, slides were incubated for 1·5 h (room temperature) with secondary goat anti-rabbit-FITC antibody (dilution of 1 : 500) in PBS and stained with Propidium iodide (final concentration: 0.23 mM) for DNA.

Statistical analysis

Data was expressed as mean ± SD. Analysis of variance (ANOVA) with the Tukey post hoc test was used for multiple comparisons. All statistics were calculated using the Statistica software (StatSoft, Tulsa, USA), and p-values <0.05 were considered significant.

Results

Determination of PS externalization

In order to assess the type of cell death induced by WP 631 in SKOV-3 cells, PS externalization (highly specific marker of early stages of apoptosis) after double staining with Annexin V-FITC and propidium iodide (PI) was analyzed. Figure 1 presents the morphological changes in SKOV-3 cells after 48h of incubation time with DOX and WP 631. Changes in the structure, size and shape of the nucleus typical for the early stages of apoptosis were observed. There was also an intense formation of apoptotic bodies. In drug-treated cells, a remarkable increase in the green fluorescence of Annexin V- FITC was visible, which indicated a translocation of PS from the inner layer of the plasma membrane to the outer layer (Figure 1A, B). Quantitative analysis of fractions of apoptotic cells (Annexin V-positive; PI-negative) and dead cells (Annexin V-positive, PI-positive; Annexin V-negative, PI-positive), is presented in Figure 2. According to the data, WP 631 induced both apoptotic and necrotic cell death, but in comparison to DOX, the percentage of apoptotic cells remained at a higher level, especially after shorter (2 h - 18% for DOX and 33% for WP 631) times of incubation. The percentage of Annexin V-positive and PI-negative cells reached the highest value at 48 h (56% for WP 631 and 48% for DOX). It is significant that at the same incubation time, the number of dead cells was more than two times higher for WP 631 (19%) than for DOX (7.7%).

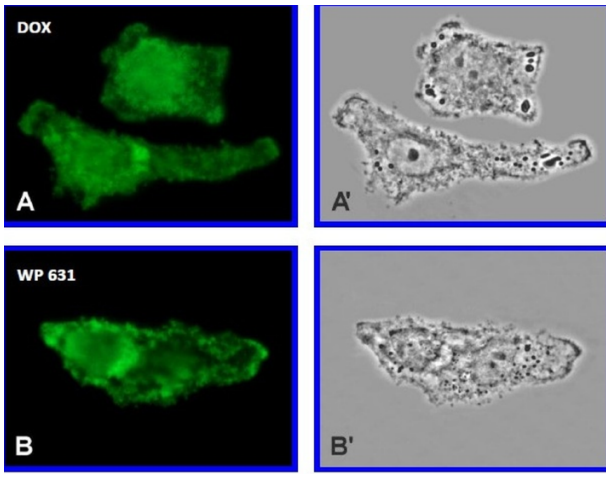

Figure 1. Fluorescence (A, B) and Phase Contrast (A', B') Images of Human SKOV-3 Ovarian Cells at 48 h after DOX and WP 631 Treatment with IC_{50} Concentrations. The cells were stained with Annexin V and visualized by fluorescence microscopy (Nikon E600, Japan), magnification 10x100

Comet assay

Figure 3 (B) displays the representative comets of the alkaline version for controls and drugs treated cells after 48 h of incubation with WP 631 and DOX. The genotoxicity effect of WP 631 and DOX, measured as the percentage of DNA in comet tail of SKOV-3 cells is shown in Figure 3 (A). Obtained quantitative results clearly demonstrated that the ovarian cancer cells treated with WP 631 reveal a higher mean level of basal DNA damage for all tested incubations times in comparison to cells treated with DOX. The comparison between the percentage of DNA in the comet tail at the beginning (2 h) and after 48 h of incubation with investigated agents indicates, that DNA damage induced by either chemical increased approximately six times. The highest percentage value of the DNA in the comet tail was observed after 48 h of incubation (43% for WP 631 and 36% for DOX). The differences between drugs were statistically significant

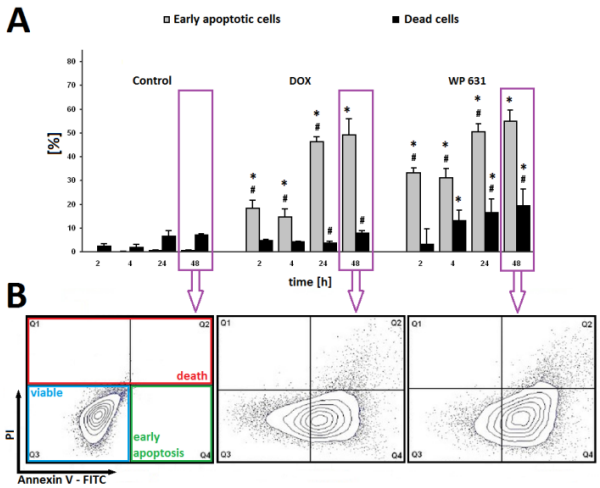

Figure 2. (A) - A comparative Study of the Effect of WP 631 and DOX on the Phosphatidylserine (PS) Externalizaction in SKOV-3 Cell Line After Double Staining with Annexin V/PI. The graph shows fraction of early apoptotic (Annexin V-positive; PI-negative) and dead cells (Annexin V-negative, PI-positive; Annexin V-positive, PI-positive) at different times (2-48 h) following treatment with IC_{50} concentration of WP 631 and DOX. (*) p<0.05 - values statistically significant in comparison to control cells, (#) p<0.05 - statistically significant differences observed between the probes incubated with WP 631 in comparison to the effect after treatment with DOX, **(B) - Determination of PS externalization after Double Staining with Annexin V/PI in human SKOV-3 Ovarian Cells.** The fraction of the viable (Q3: Annexin V-negative, PI-negative), early apoptotic (Q4: Annexin V-positive, PI-negative) and dead cells (Q1+Q2: Annexin V-negative, PI-positive; Annexin V-positive, PI-positive) after 48 h treatment with IC_{50} concentration of WP 631 and DOX are presented as typical dot plot images, obtained after flow cytometry analysis

for all investigated incubations times. It should be taken into account, that the high value of the mean error for the ovarian cancer cells after WP 631 and DOX treatment reflects probably poor diversity of highly damaged cells.

Determination of cytochrome c release

The time-course of cytochrome c (cyt c) release was estimated after incubation of SKOV-3 cells with WP 631 or DOX followed for up to 48 h. As it was shown in Figure 4, after 4 h of drug treatment, it increases the level of investigated heme protein after incubation with DOX and WP 631 (109.6% and 108.6%, respectively). However, cytochrome c level was maximal after 48 h treatment time with WP 631. At this time point, the level of cyt c in ovarian cancer cells increased to 114%. For the same experimental conditions, the percentage of cytochrome c after DOX treatment was significantly lower and did not exceed the level of control cells.

Intracellular calcium measurement

To examine whether the changes of intracellular calcium (Ca2+) were involved in apoptosis induced by WP 631, the level of intracellular calcium was studied using the fluorescence probe Fluo-4-NW. Figure 5 shows, that both drugs induced a statistically significant increase in the intracellular free calcium in the tested cells only after 48 h incubation time. At this time point, the level of intracellular calcium in the SKOV-3 cells increased by about 33% for bisintercalating anthracycline and by 47% for DOX. During the following 2-24 h treatment period, the level of Ca^{2+} remained stable (about 113% for WP 631 and 108% for DOX, respectively).

Measurment of caspase-3, -9 and -8 activity

Changes in the activities of caspases-3, -8, and 9 induced by DOX and WP 631 treatment were determined with the use of prepared sets, containing appropriate substrates. Activity of analyzed cysteine proteases has been specified after determination of protein concentration in tested samples. The final result achieved was the % of activity of specified cysteine protease, where the value of fluorescence or absorbance (depending on the method) of the control, not treated with the drug, was adopted as 100%. Experiments were conducted simultaneously with caspases-3, -8 and 9 activity inhibitors, in order to ascertain that enzymes activated by DOX or WP 631 are the tested cysteine proteases.

In the SKOV-3 cells some increase of caspase-8 and -9 activity was observed after 24 hours of incubation with DOX (178.6% for caspase-8 and 120.5% for caspase-9) and with WP 631 (130.5% for caspase-8 and 110.4% for caspase-9). These changes were statistically significant only for DOX. After 48 hours from administering the compounds, percentage of the activity of examined caspases decreased to the following values: in case of DOX - 131.8% for caspase-8 and 111% for caspase 9, and

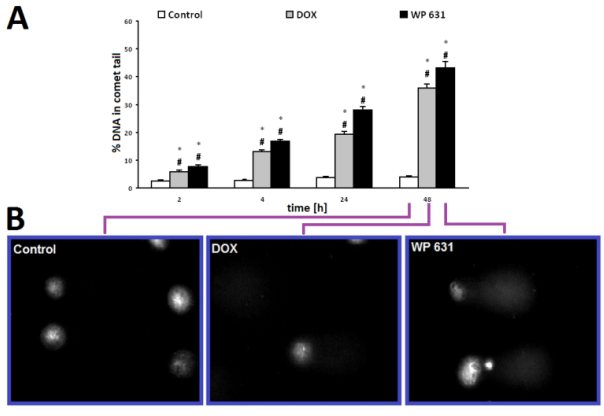

Figure 3. (A) - Tail DNA [%] of control cells and cells treated with IC_{50} concentration of WP 631 and DOX for 2, 4, 24 and 48 h in SKOV-3 cell line. The number of analyzed cells in each treatment was 50. The figure shows the mean results from three independent experiments. Error bars denote S.E.M. (*) $p<0.05$ - values statistically significant in comparison to control cells, (#) $p<0.05$ - statistically significant differences observed between the probes incubated with WP 631 in comparison to the effect after treatment with DOX. **(B) - Comet assay: representative fluorescent microscopy images of control cells and cells treated with IC_{50} concentration of WP 631 and DOX for 48 h.** DAPI stained cells were visualized under fluorescence microscope (Nikon E200 Japan), magnification 10x20

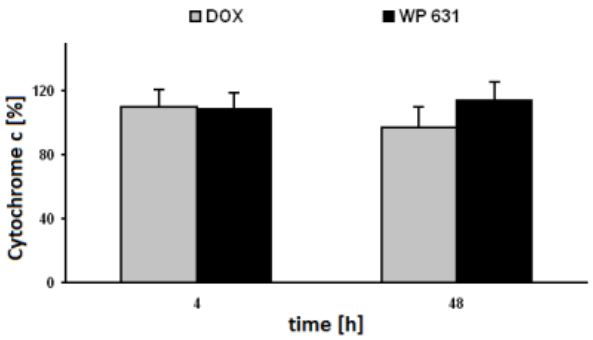

Figure 4. Changes in the Intracellular Cytochrom c level of SKOV-3 Cells Incubated with WP 631 or DOX in IC_{50} Concentration for 4 and 48 h. Absorbance of control was assumed as 100%. Results are presented as means ± S.D. of 3 experiments

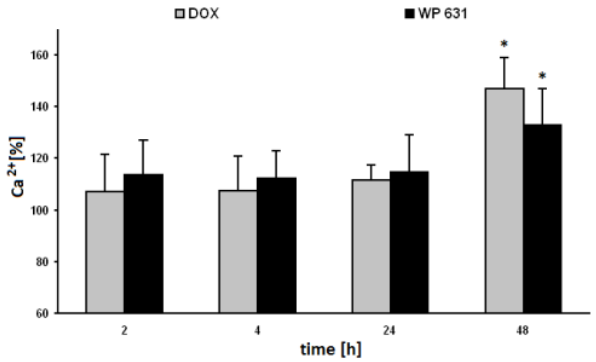

Figure 5. The Effect of WP 631 and DOX on the Ca2+ Concentration in SKOV-3 Cells. The cells were treated with an IC50 of WP 631 or DOX and then incubated for 2, 4, 24 or 48 h. The intensity of Fluo-4-NW probe fluorescence in the control cells measured, respectively after 2-48 h of incubation time, was taken as 100%. Each point represents the average ± SD of three independent experiments. (*) $p<0.05$ - values statistically significant in comparison to control cells

in relation to WP 631 - 119.8% for caspase-8 and 108.7% for caspase-9. Statistically significant changes in caspase-3 activity were observed after 24 (123.5%) and 48 (163.7%) hours of incubation of cells in the presence of DOX. In the same time range, changes induced by WP 631 were: 110.2% - 24 h and 111% for 48 h respectively (Figure 6). These changes were not statistically significant. Applied caspase-3, -8 and -9 inhibitors caused the decrease of percentage of the activity, what implied that the substrate cutting reaction was specific and resulted from the action of DOX and WP 631.

Detection of internucleosomal DNA fragmentation

To examine whether WP 631 or DOX - induced programmed cell death in tested ovarian cancer cells is related with the internucleosomal DNA fragmentation, we fractionated electrophoretically DNA extracted from the cells at various time after drugs treatment. It should be mentioned that only after DOX application to the cell culture, the characteristic DNA ladder pattern after 24 and 48 h was observed (Figure 7). Under the same conditions, no DNA fragmentation was found in untreated (control) cells as well as in WP 631 treated cells.

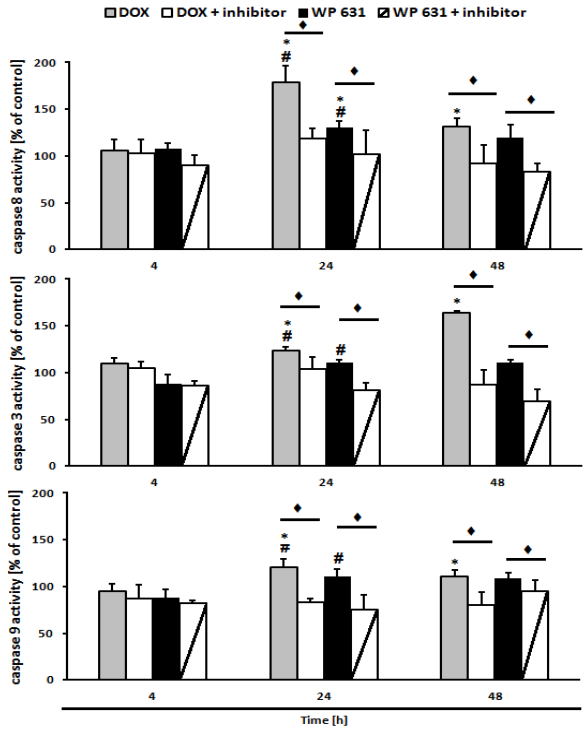

Figure 6. The Effect of WP 631 and DOX on Changes in the Activity of Caspases-8 (A), -9 (B) and -3 (C) in SKOV-3 Cells. The measurements were carried out in the presence or absence of the inhibitors. The cells were treated with an IC50 of WP 631 or DOX and then incubated for 4, 24 or 48 h. Caspases activity in control cells (without drugs treatment) measured, respectively after 2, 4, 24 and 48 h of incubation time, was taken as 100%. Each point represents the average ± SD of 3 independent experiments. (*) $p<0.05$ - values statistically significant in comparison to control cells, (#) $p<0.05$ - statistically significant differences observed between the probes incubated with WP 631 in comparison to the effect after treatment with DOX, , (♦) $p<0.05$ - statistically significant differences observed between the investigated probes in comparison to the effect after pretreatment for 1 h with the caspases inhibitors.

PARP cleavage

Both WP 631 and DOX induced cleavage of PARP (Figure 8). At the 24h time point it was clearly seen that PARP 116 kDa was cleaved into signature 85 and 25 kDa fragments. The 25 kDa fragment irreversibly binds to the broken ends of DNA, preventing the repair enzyme's to the DNA, and ensuring the irreversibility of apoptosis. During the course of WP 631 and DOX treatment, loss of the Mr 116,000 polymerase was accompanied by the appearance of an Mr ~25,000 polypeptide recognized by this antibody. Stronger expression was evidence in WP 631 case.

Immunocytochemical detection of phosphorylated H2AX histones

Representative immunofluorescence images reveal nuclear distribution of anti-γ-H2AX in SKOV-3 cells after 48 h treatment with DOX or WP 631(Figure 9). Obtained

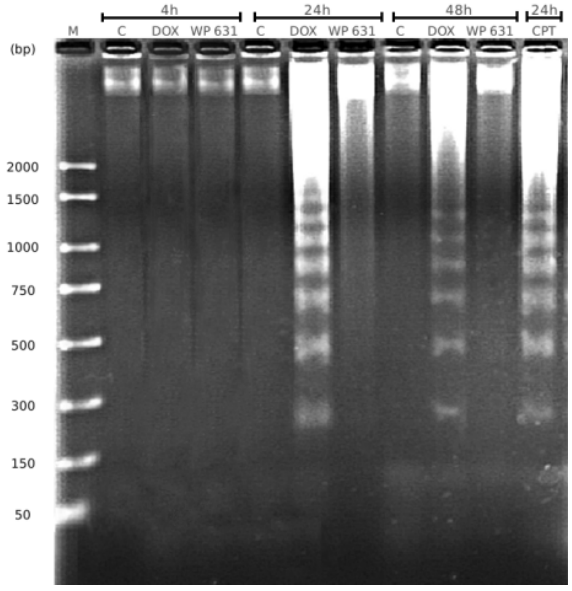

Figure 7. WP 631 or DOX - induced DNA Fragmentation detected by agarose gel electrophoresis of DNA isolated from Human Ovarian Cancer Cells. SKOV-3 cells were treated with an IC_{50} of DOX and WP 631 for 4, 24 and 48 h. (M) - PCR marker, (C) – control cells (untreated), (CPT) – positive control (cells treated with 1 μM camptothecin)

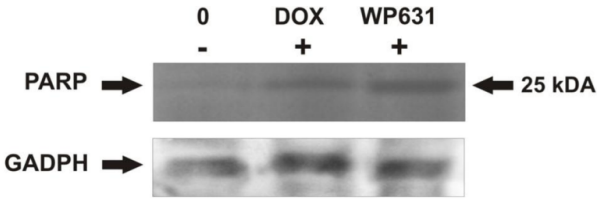

Figure 8. Western Blot Analysis Showing Cleavage of PARP in SKOV-3 Cells Upon 24 h Treatment with an IC_{50} dose of WP 631 and DOX. The expressions of PARP were detected using specific antibodies. Rabbit Anti-PARP-1 (cleaved p25) monoclonal antibody was attached to the secondary goat anti-rabbit antibody conjugated with alkaline phosphatase diluted 1/2000. Rabbit anti GAPDH antibody were used as internal controls. The blot was developed with BCIP/NBT. The panel shown is representative of three similar experiments done in triplicate

results indicated that histones H2AX were phosphorylated after treatment with both drugs. This phosphorylated form of H2AX (called γ-H2AX) has mostly been studied in association with DSB formation. However, after WP 631 treatment the higher numbers of cells showed more fluorescing anti-γ- H2AX antibodies clustered at the presumed DSB sites. Immunostaining fluorescence was also observed in cells with clear signs of apoptotic nuclear morphology (chromatin condensation).

Discussion

The current goal of cancer drug development is to identify agents that are effective cancer therapeutics while also having minimal systemic side effects (Jayashree et al., 2015). Doxorubicin (1st generation of anthracyclines) exhibits a well-established activity in gynecologic malignancies, however, its clinical application is limited due to cumulative, dose-dependent cardiotoxicity, myelosuppression or kidneys failure (Shirinbayan and Roshan, 2012; Carvalho et al., 2013). Additionally, pegylated liposomal doxorubicin (an anthracycline of the second generation) demonstrated modest efficacy in patients with platinum-resistant ovarian cancer (Suprasert et al., 2014). One of the promising alternatives to the current strategy of ovarian cancer treatment is the bisintercalating anthracycline analog - WP 631.

In this article we investigate the cell death and genotoxicity mediated by WP 631 in SKOV-3 cells. DNA damage - both exogenous and endogenous - generated by

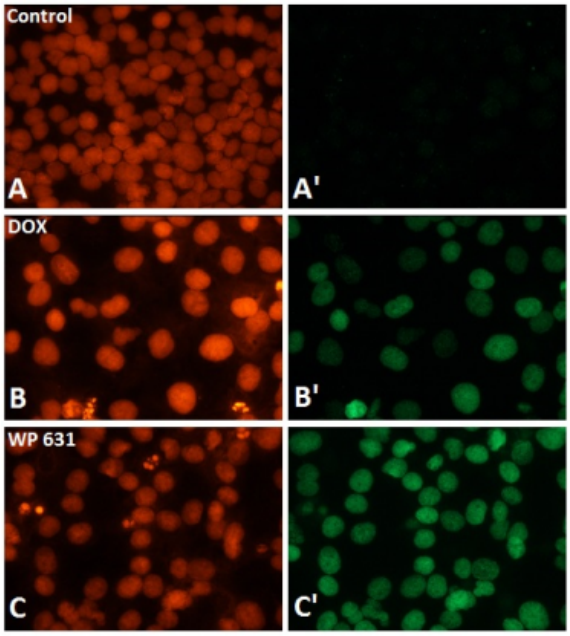

Figure9. Immunocytochemical Detection of γ-phosphorylated H2AX Histones in SKOV-3 Control Cells. (A'), after 48h treatment with DOX at IC_{50} concentrations (B') or WP 631 at IC_{50} concentrations (C'). A, B, C - Cells were stained with propidium iodide for DNA (red fluorescence). A', B', C' - The cells were stained with primary rabbit polyclonal antibody raised against γ-human H2AX histones phosphorylated at Ser139 and secondary goat anti-rabbit IgG - FITC antibody (green fluorescence). Cells were visualized by fluorescence microscopy (Nikon E600, Japan), magnification 10x100

direct and indirect interaction of the drugs with the double helix - plays the fundamental role in the mechanism of the action of anthracyclines drugs. Degradation of DNA can be caused by single- and double-stranded DNA breaks arising through the interaction of free radicals generated in the anthracycline redox cycle with the sugar backbone of DNA and inhibition of topoisomerase I and /or II (Szwed and Jozwiak, 2014).

In this study, the alkaline version of comet assay (pH>13) was performed to measure the DNA damage. This method allows detection of single and double-stranded DNA breaks, DNA fragmentation induced by free radicals, cross-type DNA-DNA bonds or DNA-protein interactions (Leangie et al., 2015). The obtained results show that WP 631 was considerably more genotoxic towards the investigated cell line than DOX. This effect was especially visible after longer times of incubation. The higher level of DNA damage may result from the fact that WP 631 exhibits extremely high DNA binding affinity ($K = 2.7\times10^{11}M^{-1}$) in comparison to the monomeric anthracyclines, e.g. DOX ($K=2\times10^{5}\ M^{-1}$). The binding constant for WP 631 is close to that of various transcriptional factors. Thus, it can be used in much lower concentrations than DOX or DNR in cancer treatment (Portugal et al., 2005). Our earlier studies established that IC_{50} for WP 631 was three times lower than for DOX in the SKOV-3 cell line tested in this article (Rogalska et al., 2011).

In our study, we supplemented the comet assay method with a visualization of the immunocytochemical detection of phosphorylated H2AX histones. H2AX phosphorylation at serine 139 (γ-H2AX) is a sensitive indicator of DNA damage. Histone H2AX becomes rapidly phosphorylated to yield to a form known as γ-H2AX in response to double-strand DNA damage. Mei's group suggested that the expression of phosphorylated H2AX may play an important role in the development and prognosis of epithelial ovarian cancer. In these authors' studies, among the sensitive cases, a high expression of phosphorylated H2AX was found in 53.2% cases while for resistant cases, the high expression rate was 80% (Mei et al., 2015). A high expression of phosphorylated H2AX was found in 53.2% of sensitive cases while for resistant cases, the high expression rate was 80% (Mei et al., 2015). Our data demonstrated that 48 h exposure of cells to WP 631 led to an increase in γH2AX to a greater extent than DOX. As shown in Figure 9, the nuclear chromatin present in the apoptotic bodies or in the fragmented nuclei of apoptotic cells was very distinctive due to the highly intense immunofluorescence of γH2AX reflecting the concentration of the foci. This immunofluorescent foci represents DNA damage that involves the formation of DSBs (DNA Double-Strand Breaks) caused by these drugs. DSB lesions are recognized by the cell as lethal and trigger apoptosis (Ikeda et al., 2010).

The comet assay method presented in this paper does not give an unambiguous answer to the question of whether DNA breaks are the result of the mobilization of apoptotic cell death machinery, because DNA is also degraded in necrotic (dead) cells (Surova and Zhivotovsky, 2013). Therefore, we examined the type of cell death

induced by WP 631 and DOX in SKOV-3 cells. It is well known that the mechanism of the induction of the cell death of the first and second generation of anthracyclines is pleiotropic (Rochette et al., 2015) and depends on the cell line type. It has been suggested that apoptosis plays an important role in the cytotoxic effects of anthracycline antibiotics in cells derived from solid tumors as well as in leukemic cells (Szwed et al., 2014, Marczak et al., 2015).

One of the most important markers analyzed in studies of apoptosis is phosphatidylserine (PS) externalization. The maintenance of transbilayer lipid asymmetry is essential for normal cell membrane functions and the homeostasis of organisms. Loss of asymmetric distribution of lipids leads to changes in the physical properties of the membrane, which in turn are reflected in the cell - cell and membrane - intracellular proteins' interactions. Translocation of PS from the internal to external surface of the plasma membrane appears to be one of the important mechanism by which apoptotic cells are recognized and eliminated by phagocytic macrophages (Kimani et al., 2014).

The quantitative flow cytometry analysis performed in this study, and our previous measurements with double staining Hoechst 33250/propidium iodide (Rogalska et al., 2011) indicated that the major mode of cell death induced by WP 631 was apoptosis. However, after prolonged WP 631 treatment time (48h), a significant population of cells with features of cell death (PI positive population of cells) was also observed. In studies related to the movement of PS, a lot of attention is placed on the role of reactive oxygen species. There are reports indicating that the cause of the movement of PS may be a process of oxidation of the phospholipids (Catala, 2015). Our previous study showed that the tested analog of anthracyclines, in comparison to DOX, induced a significantly higher level of ROS. Additionally, the apoptosis was mediated by reactive oxygen species, owing to the addition of antioxidant resulting in a statistically significant decrease in the level of apoptotic and necrotic cells. Moreover, we conclude that apoptotic cell death was associated with morphological changes and a decrease in mitochondrial membrane potential (Rogalska et al., 2011). On the basis of these results, we expected to detect the mentioned below markers of apoptosis related to an internal pathway.

The Yamashita group suggested that the oxidation and subsequent externalization of PS is likely to involve cytochrome c (Yamashita et al., 2012). Cytochrome c takes part in energy production in the cells and its contribution is also confirmed in apoptosis, during which it escapes from the mitochondria to the cytoplasm and forms, together with the factor Apaf-1, apoptosom. The strong interaction between cytochrome c and PS externalization has been confirmed (Yamashita et al., 2012; Kimani et al., 2014). The increase of PS observed over time on the cell surface was correlated with an increase in the quantity of cytochrome c that occurs in the cytosol in many experiments (Xue et al., 2014). Our results confirm that both drugs were able to enhance the level of cytochrome c (by about 10-15% in comparison to control), however, these changes were not statistically significant. The obtained results were correlated with the externalization of PS. After the same time of incubation (48 h) with both drugs, the largest percentage of apoptotic cells was also seen (Annexin-V positive and PI negative population of cells).

Phosphatidylserine exposure may also be induced by a rapid increase in intracellular free calcium ions (Kmit et al., 2013; Weisthal et al., 2014). Several studies have shown higher levels of Ca^{2+} in the activation and execution of cell death (Parrish et al., 2013). Other data indicate that such PS displacement has been shown to be reversible if extracellular Ca^{2+} is chelated after PS externalization (Verhoven et al. 1999). Calcium ions may also activate scramblases, which transport cell membrane lipids passively in both directions. For this reason they are partially involved in PS externalization (Suzuki et al., 2013). It is well known that the first generation of anthracyclines (DOX) causes chronic cardiotoxicity, induced by cellular calcium homeostasis deregulation (Joshi et al., 2015), but the mechanism of the action of the bisintercalating anthracyclines analog, including the role of calcium ions administration, is still under debate. Therefore, the next stage of our study was to determine the intracellular calcium ion level after treatment with WP 631. Our results clearly demonstrate that analog, similarly to DOX, was able to significantly increase the level of Ca^{2+} in SKOV-3 cells, but only after a longer time (48 h) of incubation. It is worth noting that DOX induced greater changes in the level of calcium ions than WP 631.

In this paper, the assessment of apoptosis induced by WP 631 was carried out in terms of caspases participation in the process of programmed cell death. It is well known that the presence of active caspases have been shown to play an important role in the apoptotic cell death induced by anticancer drugs. Analysis of cysteine proteases activity was initiated by examining the level of the activation of caspases -8 and -9, participating in the extrinsic and the mitochondrial pathway of apoptosis respectively (Goldar et al., 2015). We also examined the activation of caspase-3, the chief executioner of programmed cell death.

In the literature, it is described that caspase-8 and -3 are direct activators of apoptosis. A strong correlation between the activity of both enzymes was observed by Rogalska (Rogalska et al., 2010), who showed a direct relationship between the activity of caspase-8 and -3 in A549 and MCF-7 cells treated with aclarubicin (ACL). In this study we have also noticed the time-dependent correlation between the activation of caspase-8 and -3 only in DOX treatment probes. The novel bisanthracycline was able to increase only the activity of caspase-8 (24 h incubation time). The SKOV -3 cells, even in the presence of cytosol cytochrome c and deoxyadenosine triphosphate, have a dysfunctional apoptosome activity. The SKOV3 cells retain the ability to form the Apaf-1 oligomer, however, there is a diminished amount of caspase-9 in the apoptosome (Liu et al., 2002). This could be the reason for the deficiency of caspase-9 and caspase-3 observed in our experiments. This indicates the different mechanism of the drug's action depending on the type of ovarian cell line. Our previous study reveals that WP 631 is able to induce caspase - dependent apoptosis in ovarian cancer cell line (OV-90) derived from the malignant ascites of a patient

diagnosed with advanced disease (Gajek et al., 2014).

The obtained results suggest that, besides caspase-3, not only may other effectors such as caspase-6 or caspase-7 be responsible for apoptotic changes, but also other agents acting independently of them. In order to extend the data on the differences in the mechanisms that lead to cell death after treatment with DOX and WP 631, we studied the PARP cleavage and DNA degradation.

Most studies indicate that proteolytically active caspase-3 can cleave a number of cellular proteins, such as PARP, DFF45 (ICAD, DNA fragmentation factor), resulting in morphological features and DNA fragmentation into low molecular weight fragments. After treatment with DOX, all three tested caspases were activated. The PARP cleavage and the DNA ladder was also observed. However, in the cells incubated with analog, only the increase in the activity of caspase-8 was statistically significant. We did not observe typical DNA fragmentation, but we noted the PARP cleavage. Most probably, these effects are connected with the activation of caspases. There are a few articles confirming the engagement of caspase-8 in the PARP cleavage (Garnier et al., 2003; Treude et al., 2014). Caspase-3 is not the only protein capable of cutting PARP. This protein can be cleaved and inactivated by caspase-3, caspase-7, and calpains (Boucher et al., 2012; Ko and Ren, 2012). In our studies caspase-8 was activated in the case of both drugs, and it is probably involved in PARP cleavage.

The present study provides further information which explains the series of events induced in cell nucleus by WP 631. The results obtained clearly demonstrate that the ovarian cancer cells treated with WP 631 show a higher mean level of basal DNA damage in comparison to DOX. We have shown that apoptosis is the prevalent form of cell death at early time points by newer derivatives of anthracyclines. Recent studies demonstrate the involvement of caspase-independent pathways in the cell death induced by several cytotoxic agents (Kim et al., 2014; Lee et al., 2014). The outcome of the cellular response appears to be dependent on the type and dose of chemotherapeutic stress within the cellular context. Moreover, inhibition of the major apoptotic routes and direct blockade of caspases failed to protect against the cytotoxic effects of WP 631 in SKOV-3 cells.

Acknowledgements

This study was supported by grant Nr N N405 100939 of Ministry of Science and High Education (Poland)

References

Boucher D, Blais V, Denault JB (2012). Caspase-7 uses an exosite to promote poly (ADP ribose) polymerase 1 proteolysis. *Proc Natl Acad Sci U S A*, **15**, 5669-74.

Carvalho FS, Burgeiro A, Garcia R, et al (2014). Doxorubicin-Induced Cardiotoxicity: From Bioenergetic Failure and Cell Death to Cardiomyopathy. *Med Res Rev*, **34**, 106-35.

Catalá Á (2015). Lipid peroxidation modifies the assembly of biological membranes "The Lipid Whisker Model". *Front Physiol*, **5**, 520.

Chaopotong P, Therasakvichya S, Leelapatanadit C, et al (2015). Ovarian cancer in children and adolescents: treatment and reproductive outcomes. *Asian Pac J Cancer Prev*, **11**, 4787-90.

Fujiwara K, Kurosaki A, Hasegawa K (2013). Clinical trials of neoadjuvant chemotherapy for ovarian cancer: what do we gain after an eortc trial and after two additional ongoing trials are completed? *Curr Oncol Rep*, **3**, 197-200.

Gajek A, Denel M, Bukowska B, et al (2014). Pro-apoptotic activity of new analog of anthracyclines-WP 631 in advanced ovarian cancer cell line. *Toxicol In Vitro*, **2**, 273-81.

Garnier P, Ying W, Swanson RA (2003). Ischemic preconditioning by caspase cleavage of poly(ADP-ribose) polymerase-1. *J Neurosci*, **22**, 7967-73.

Goldar S, Khaniani MS, Derakhshan SM, et al (2015). Molecular mechanisms of apoptosis and roles in cancer development and treatment. *Asian Pac J Cancer Prev*, **16**, 2129-44.

Ikeda M, Kurose A, Takatori E, et al (2010). DNA damage detected with γH2AX in endometrioid adenocarcinoma cell lines. *Int J Oncol*, **5**, 1081-88.

Jayashree BS, Nigam S, Pai A, et al (2015). Targets in anticancer research-A review. *Indian J Exp Biol*, **8**, 489-507.

Jiménez IJ, Garcia Casado Z, Palanca Suela S, et al (2013). Novel and recurrent BRCA1/BRCA2 mutations in early onset and familial breast and ovarian cancer detected in the program of genetic counseling in cancer of valencian community (eastern Spain). Relationship of family phenotypes with mutation prevalence. *Fam Cancer*, **4**, 767-77.

Joshi M, Sodhi KS, Pandey R, et al (2015). Duxorubicin-induced cardiotoxicity. *Int J Basic Clin Pharmacol*, **1**, 6-14.

Kim EA, Jang JH, Lee YH, et al (2014). Dioscin induces caspase-independent apoptosis through activation of apoptosis-inducing factor in breast cancer cells. *Apoptosis*, **7**, 1165-75.

Kimani SG, Geng K, Kasikara C, et al (2014). Contribution of Defective PS Recognition and Efferocytosis to Chronic Inflammation and Autoimmunity. *Birge Front Immunol*, **5**, 566.

Kmit A, van Kruchten R, Ousingsawat J, et al (2013). Calcium-activated and apoptotic phospholipid scrambling induced by Ano6 can occur independently of Ano6 ion currents. Cell Death and Disease. *Cell Death Dis*, **4**, 611.

Ko HL, Ren EC (2012). Functional Aspects of PARP1 in DNA repair and transcription. *Biomolecules*, **2**, 524-48.

Lee K, Hart MR, Briehl MM, et al (2014). The copper chelator ATN-224 induces caspase-independent cell death in diffuse large B cell lymphoma. *Int J Oncol*, **1**, 439-47.

Liu JR, Opipari AW, Tan L, et al (2002). Dysfunctional apoptosome activation in ovarian cancer: implications for chemoresistance. *Cancer Res*, **3**, 924-31.

Marczak A, Denel-Bobrowska M, Lukawska M, et al (2015). Formamidinodoxorubicins are more potent than doxorubicin as apoptosis inducers in human breast cancer cells. *Anticancer Res*, **4**, 1935-40.

Mei L, Hu Q, Peng J, et al (2015). Phospho-histone H2AX is a diagnostic and prognostic marker for epithelial ovarian cancer. *Int J Clin Exp Pathol*, **5**, 5597-602.

Pal S, Ahir M, Sil PC (2012). Doxorubicin-induced neurotoxicity is attenuated by a 43-kD protein from the leaves of Cajanus indicus L. via NF-κB and mitochondria dependent pathways. *Free Radic Res*, **6**, 785-98.

Parrish AB, Freel CD, Kornbluth S (2013). Cellular mechanisms controlling caspase activation and function. *Cold Spring Harb Perspect Biol*, **5**, 8672.

Portugal J, Cashman DJ, Trent JO, et al (2005). A new bisintercalating anthracycline with picomolar DNA binding affinity. *J Med Chem*, **48**, 8209-19.

Pradjatmo H, Dasuki D, Anwar M, et al (2014). Methylation status and immunohistochemistry of BRCA1 in epithelial

ovarian cancer. *Asian Pac J Cancer Prev*, **21**, 9479-85.
Rochette L, Guenancia C, Gudjoncik A, et al (2015). Anthracyclines/trastuzumab: new aspects of cardiotoxicity and molecular mechanisms. *Trends Pharmacol Sci*, **6**, 326-48.
Rogalska A, Gajek, Szwed M, et al (2011). The role of reactive oxygen species in WP 631-induced A death of human ovarian cancer cells: a comparison with the effect of doxorubicin. *Toxicol In Vitro*, **8**, 1712-20.
Rogalska A, Szwed M, Jozwiak Z (2010). Aclarubicin-induced apoptosis and necrosis in cells derived from human solid tumours. *Mutat Res*, **700**, 1-10.
Shirinbayan V, Roshan VD (2012). Pretreatment effect of running exercise on HSP70 and DOX-induced cardiotoxicity. *Asian Pac J Cancer Prev*, **11**, 5849-55.
Siegel R, Naishadham D, Jemal A (2013). Cancer statistics. *CA Cancer J Clin*, **63**, 11-30.
Sundar S, Neal RD, Kehoe S (2015). Diagnosis of ovarian cancer. *BMJ*, **1**, 351-4443.
Suprasert P, Manopunya M, Cheewakriangkrai C (2014). Outcomes with single agent LIPO-DOX in platinum-resistant ovarian and fallopian tube cancers and primary peritoneal adenocarcinoma - Chiang Mai University Hospital experience. *Asian Pac J Cancer Prev*, **3**, 1145-8.
Surova O, Zhivotovsky B (2013). Various modes of cell death induced by DNA damage. *Oncogene*, **32**, 3789-97.
Suzuki J, Fujii T, Imao T, et al (2013). Calcium-dependent Phospholipid Scramblase Activity of TMEM16 Protein Family Members. *J Biol Chem*, **19**, 13305-16.
Szwed M, Jozwiak Z (2014). Genotoxic effect of doxorubicin-transferrin conjugate on human leukemia cells. *Mutat Res Genet Toxicol Environ Mutagen*, **771**, 53-63.
Szwed M, Laroche-Clary A, Robert J, et al (2014). Induction of apoptosis by doxorubicin-transferrin conjugate compared to free doxorubicin in the human leukemia cell lines. *Chem Biol Interact*, **220**, 140-8.
Treude F, Kappes F, Fahrenkamp D, et al (2014). Caspase-8-mediated PAR-4 cleavage is required for TNFα-induced apoptosis. *Oncotarget*, **10**, 2988-98.
Verhoven B, Krahling S, Schlegel RA, et al (1999). Regulation of phosphatidylserine exposure and phagocytosis of apoptotic T lymphocytes. *Cell Death Differ*, **3**, 262-70.
Weisthal S, Keinan N, Ben-Hail D, et al (2014). Ca(2+)-mediated regulation of VDAC1 expression levels is associated with cell death induction. *Biochim Biophys Acta*, **10**, 2270-81.
Wojcik T, Buczek E1, Majzner K, et al (2015). Comparative endothelial profiling of doxorubicin and daunorubicin in cultured endothelial cells. *Toxicol In Vitro*, **3**, 512-21.
Xue X, Yu JL, Sun DQ, et al (2014). Curcumin induces apoptosis in SGC-7901 gastric adenocarcinoma cells via regulation of mitochondrial signaling pathways. *Asian Pac J Cancer Prev,* **9**, 3987-92.
Yamashita A, Morikawa H, Tajima N, et al (2012). Mechanisms Underlying Production And Externalization of Oxidized Phosphatidylserine in Apoptosis: Involvement of Mitochondria. *Yonago Acta Med*, **1**, 11-20.
Yang F, Teves SS, Kemp CJ, et al (2014). Doxorubicin, DNA torsion, and chromatin dynamics. *Biochim Biophys Acta*, **1**, 84-9.
Zabka A, Trzaskoma P, Maszewski J (2013). Dissimilar effects of β-lapachone- and hydroxyurea-induced DNA replication stress in root meristem cells of Allium cepa. *Plant Physiol Biochem*, **73**, 282-93.
Zhao D, Wu LY, Wang XB, et al (2015). Role of neoadjuvant chemotherapy in the management of advanced ovarian cancer. *Asian Pac J Cancer Prev*, **6**, 2369-73.